Electronic Supplementary Information

Simultaneously Achieving Thermal Insulation and Rapid Water Transport in Sugarcane Stems for Efficient Solar Steam Generation

Jie Liu,[a] Qinglei Liu,*[a] Dongling Ma,*[b] Yang Yuan,[a] Jiahao Yao,[c] Wang Zhang,[a] Huilan Su,[a] Yishi Su,[a] Jiajun Gu,*[a] and Di Zhang[a]

[a] *State Key Laboratory of Metal Matrix Composites, Shanghai Jiao Tong University, Shanghai 200240, China*

[b] *Institut National de la Recherche Scientifique (INRS), Centre Énergie Materiaux et Télécommunications, Université du Québec, Québec J3X 1S2, Canada*

[c] *Shanghai Foreign Language School, Shanghai 200083, China*

**E-mail: liuqinglei@sjtu.edu.cn (Q. L. L.); ma@emt.inrs.ca (D. L. M.); gujiajun@sjtu.edu.cn (J. J. G.)*

Contents:

1. UV-*vis* absorption contrast for the surface carbonized sugarcane and the powders of the carbonized sugarcane.

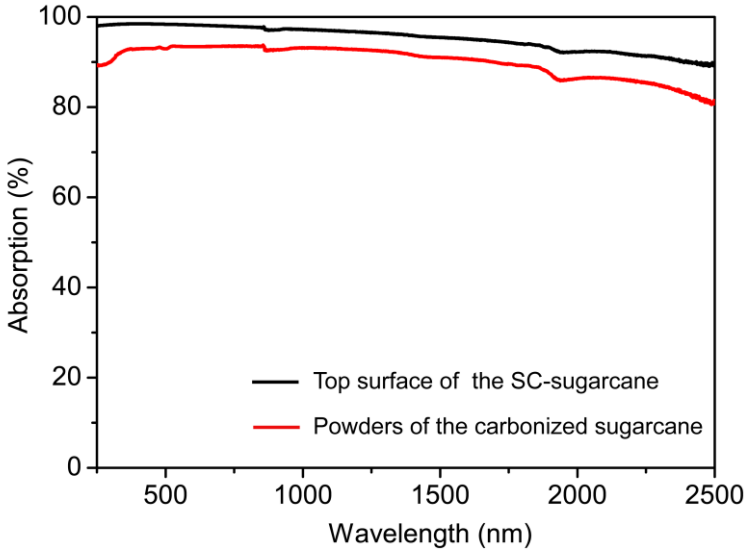

Figure S1. UV-*vis* absorption of the carbonized surface sliced from surface carbonized sugarcane and the powders of the carbonized sugarcane, respectively.

2. Experimental evidence for the accessibility of two kinds of pores to water.

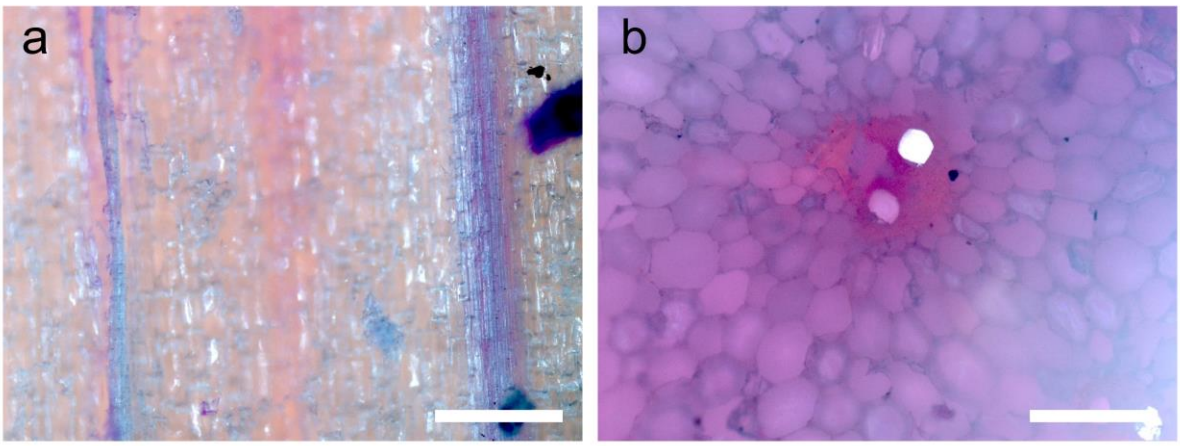

Figure S2. Longitudinal (a) and cross section (b) optical images of the SC-sugarcane stem after an impregnation process using a rhodamine B water solution (0.1mg mL^{-1}). Scale bars: 200 μm.

3. Pore size distribution of the sugarcane.

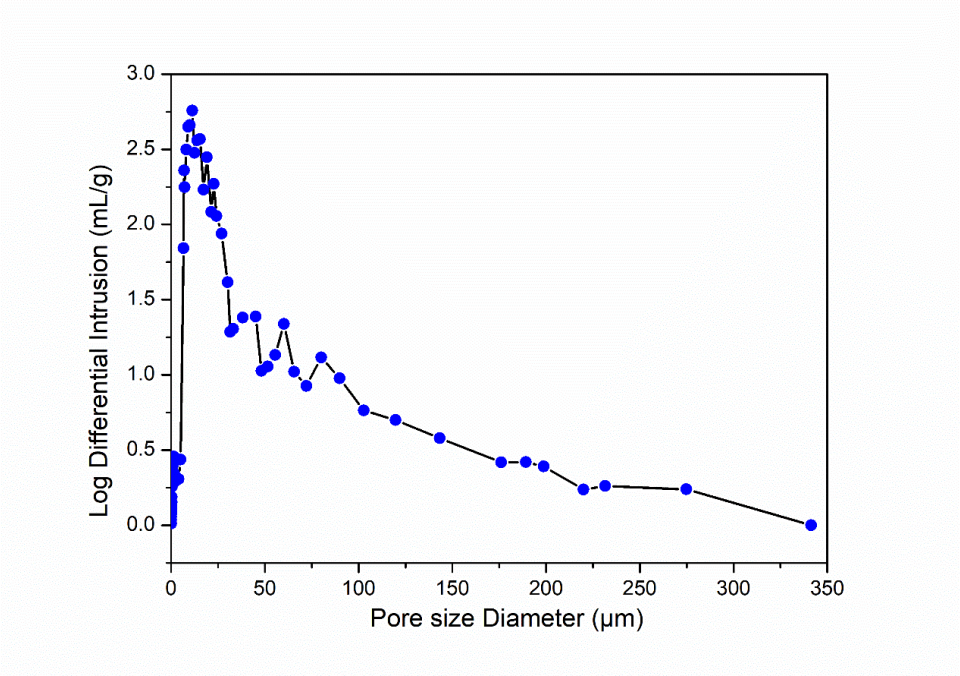

Figure S3. Pore size distribution of the freeze-dried sugarcane measured with mercury-injection method.

4. Reflectance spectrum of the SC-sugarcane

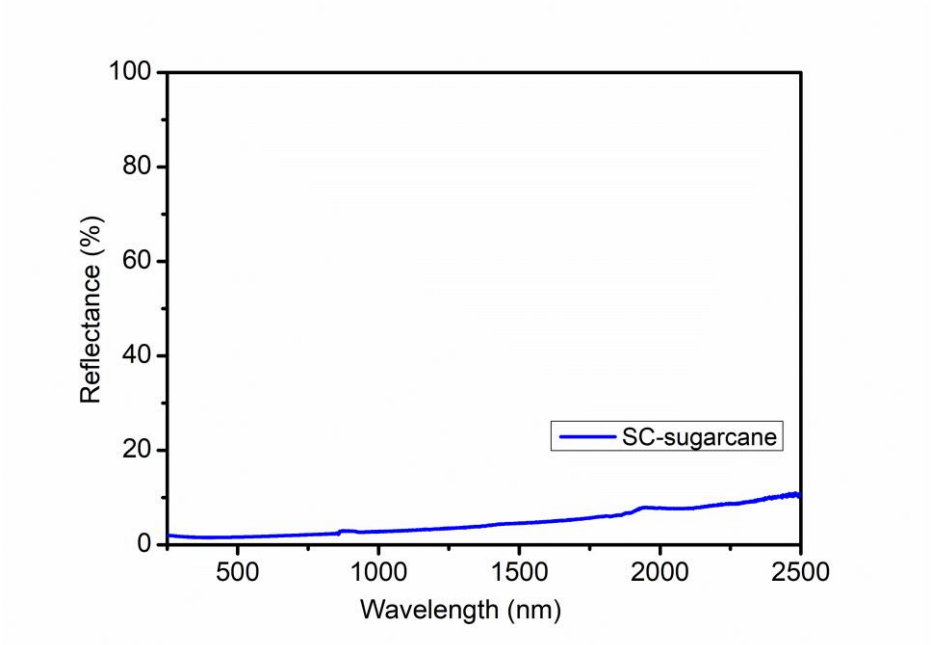

Figure S4. Reflectance spectrum of the SC-sugarcane.

5. Calculation for the closed cell ratio and open cell ratio.

$$D = \rho_0 / \rho \quad (1)$$

$$P = 1 - D \quad (2)$$

$$P_C = 1 - P_O \quad (3)$$

where the D is the dense degree, ρ_0 is the bulk density, ρ is the true density, P is the porosity, P_O and Pc are the open and closed porosities that represent the volume percentages of the vascular bundles and the parenchyma cells, respectively.

Table S1. Open and closed porosity of the SC-sugarcane.

Bulk density [a] (ρ_0)	True density [b] (ρ)	Dense degree (D)	Porosity (P)	Open porosity [a] (P_O)	Closed porosity (P_C)
0.244 g cm^{-3}	1.685 g cm^{-3}	0.145	85.5 %	41.0 %	44.5 %

[a] mercury porosimetry analysis; [b] gas pycnometry analysis.

6. Thermal conductivity calculation.

The thermal conductivity of the surface-carbonized sugarcane was measured and calculated by equation $\kappa = \rho * \alpha * C$, where ρ is the density, which was calculated from the weight and volume; α is the thermal diffusivity, which was measured by a Netzsch LFA 447 Nanoflash, and C is the specific heat capacity, which was measured by differential scanning calorimetry (DSC, Perkin Elmer DSC8000). The sample size is 1×1 cm, thickness t <2 mm.

Table S2. Thermal conductivity determination for the surface-carbonized sugarcane.

State	Density (ρ)	Thermal diffusivity (α)	Specific heat capacity (C)	Thermal conductivity (κ)
Wet	0.415 g cm^{-3}	0.233 mm^2 s^{-1}	2.287 J g^{-1} K^{-1}	0.221 W m^{-1} K^{-1}
Dry	0.244 g cm^{-3}	0.244 mm^2 s^{-1}	1.353 J g^{-1} K^{-1}	0.081 W m^{-1} K^{-1}

7. Optimization of the SC-sugarcane's thickness.

To optimize the water transport distance and thermal insulation during the solar steam generation, we systematically studied the evaporation efficiency of the SC-sugarcane with different thickness (Figure S5). In our experiment, the mass changes of the samples with thickness of 1.8 cm and 2.3 cm were higher than that in the sample whose thickness was 1.0 cm under 1 sun illumination for 1 h (Figure S5a). Because the performance under 1 sun was nearly the same for the samples with thickness of 1.8 and 2.3 cm, we further investigated their performance under 2 sun illumination. The results showed that the mass change of water was much higher when the sample thickness was 1.8 cm, reflecting the good match of the water evaporation rate with water transmission (Figure S5b). Infrared (IR) thermal images (Figure S5c) demonstrated that the surface temperature of the 2.3 cm-thick sugarcane was 97 °C, which is much higher than that (51 °C) of the 1.8 cm-thick sample. Straightforwardly it would be expected that with a higher surface temperature, the water evaporation would be more rapid and thereby higher mass change for the 2.3 cm-thick sample, which is however opposite to the observed mass change results. This is because although the thermal insulation got better with the thickness increase, the distance that water was to transfer also became longer. This decreases the water supply and suppresses the water evaporation. Herein, the optimized thickness of our sugarcane sample is 1.8 cm.

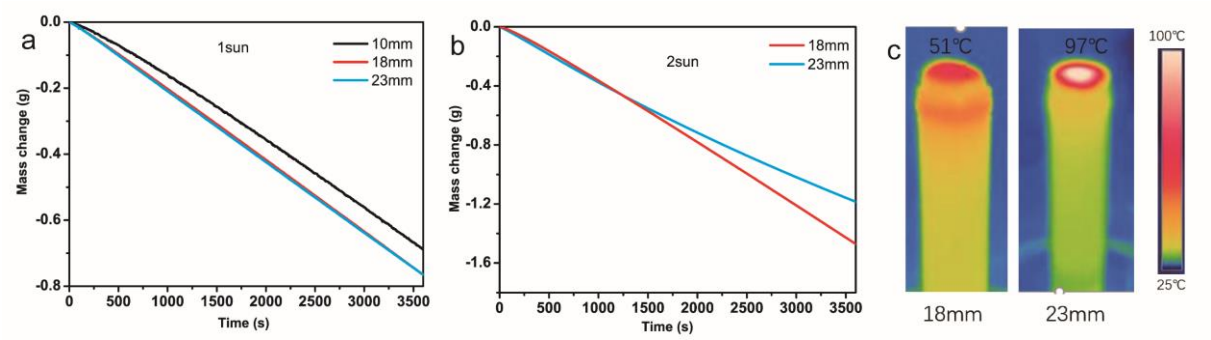

Figure S5. Mass change of water with SC-sugarcane over time at an optical density (a) of 1 kW m^{-2} (1 sun) and (b) 2 kW m^{-2} (2 sun); (c) IR images of the 1.8 cm and 2.3 cm thick samples under 2 kW m^{-2}. The optimized thickness was found to be 1.8 cm.

8. Temperature rises of the SC-sugarcane.

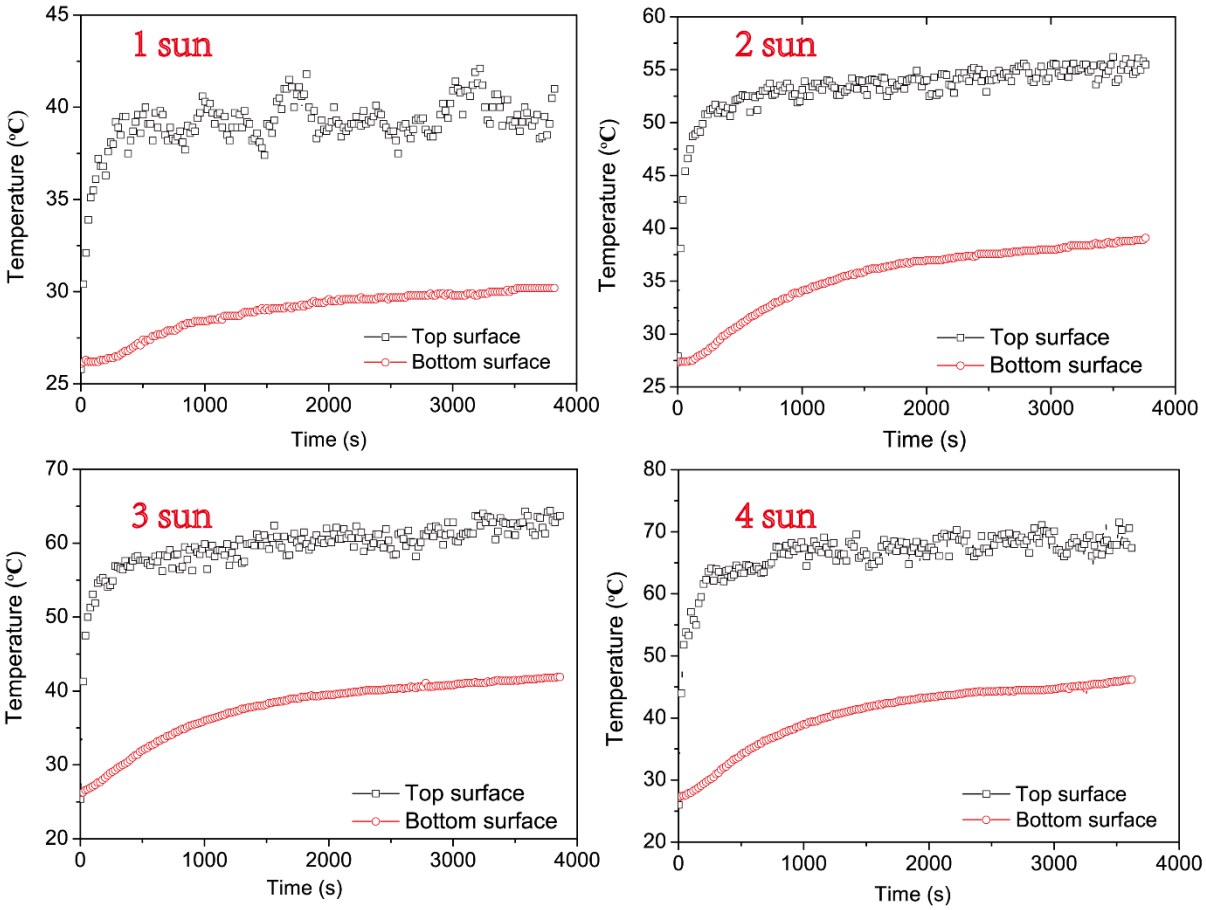

Figure S6. Increase of temperature of the top and bottom surface of SC-sugarcane as a function of illumination time under solar illumination of 1, 2, 3, and 4 kW m^{-2}.

9. IR image of the blank water under 1 sun illumination for 1 hour.

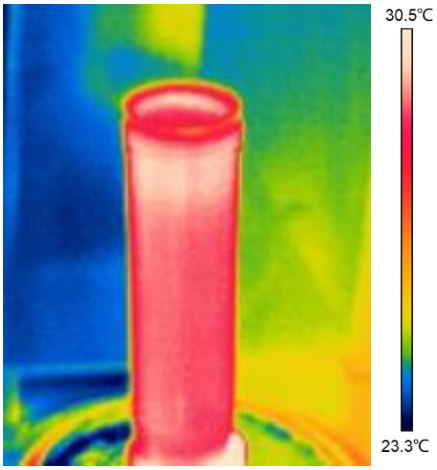

Figure S7. IR image of water under 1 sun irradiation for 60 min. The average temperature of the surface is 29.5 °C and that of the bulk is 29.4 °C.

10. Infrared photos of the SC-sugarcane illuminated for different time.

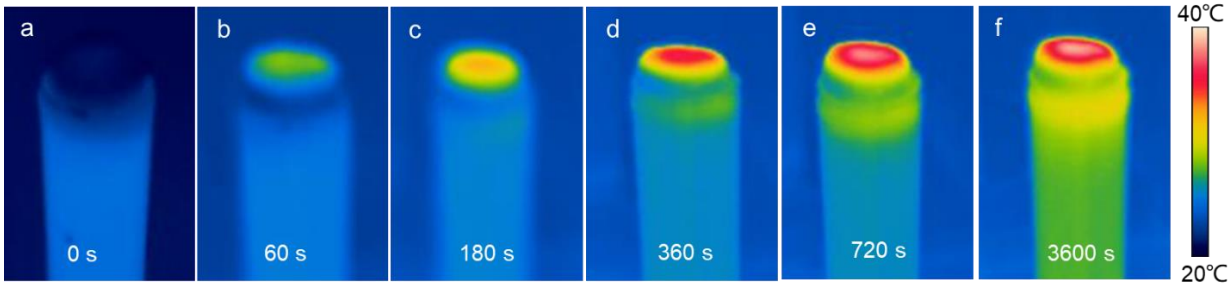

Figure S8. Infrared photos of the surface carbonized sugarcane in the process of solar vapor generation (1 kW m^{-2}) for 0, 60, 180, 360, 720, and 3600 s, respectively.

11. Photographs of SC-sugarcane-based systems for solar steam generation.

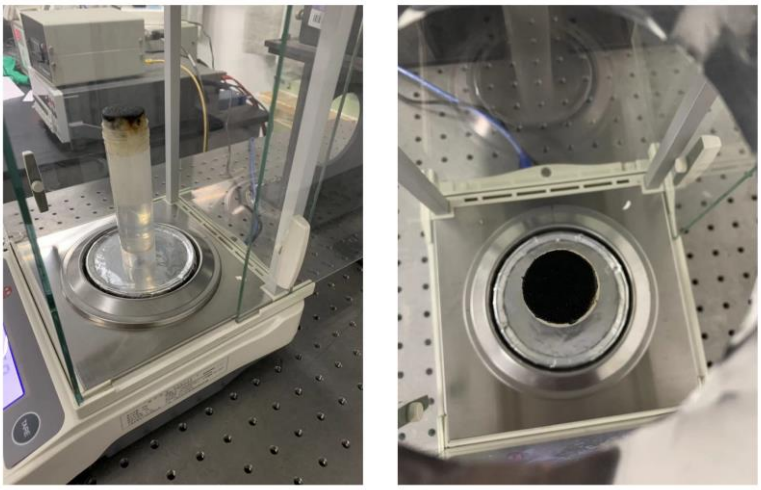

Figure S9. Photographs of SC-sugarcane-based systems for solar steam generation.

12. Contrast experiment of wood-based samples on the same test system.

We prepared the SC-wood (basswood) by heating the wood surface with an alcohol lamp for 2 min to carbonize its surface. This process is the same to that for SC-sugarcane. Both the wood and sugarcane have the same thickness (2 cm). Figure S10a and b indicate that the evaporation rate and efficiency of SC-sugarcane are higher than those of SC-wood. IR images (Figure S10c) show that the surface temperature of the SC-sugarcane is much higher that the SC-wood, showing the better thermal insulation properties of the SC-sugarcane.

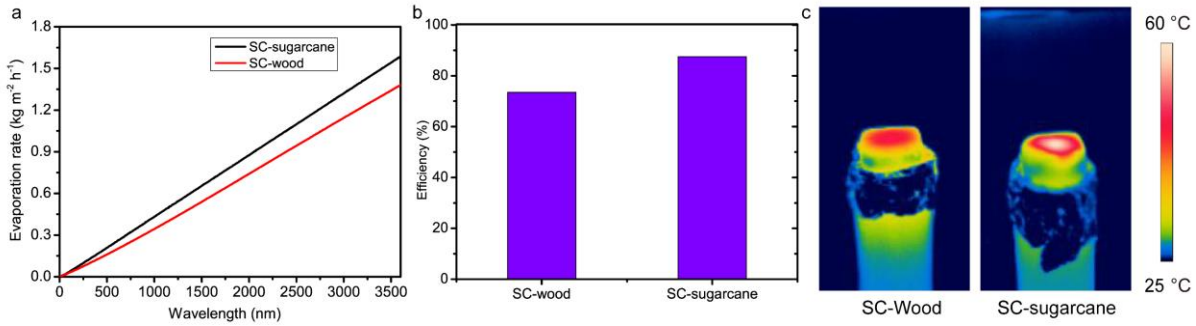

Figure S10. (a) Evaporation rate and (b) efficiency of SC-sugarcane and SC-wood over time at an optical density of 1 kW m^{-2} (1 sun); (c) IR images of the 2-cm-thick SC-sugarcane and SC-wood samples under 1 kW m^{-2} after 1 h illumination.

13. SI-1: COMSOL simulation of temperature distribution and water flow velocity in sugarcane.

The 2D geometry shown below represents the microstructural unit of the sugarcane (340×300 μm^2), the vascular bundle contains two parts, one is the vessel (d_v~60 μm) and the other is the sieve tubes (d_t~20 μm) surrounding the vessel connected by pits (d_p~4 μm). The surrounding of the sieve tubes is the parenchyma cells (d_c~100 μm, h~300 μm) connected with pores (d~1 μm) (Figure S11).

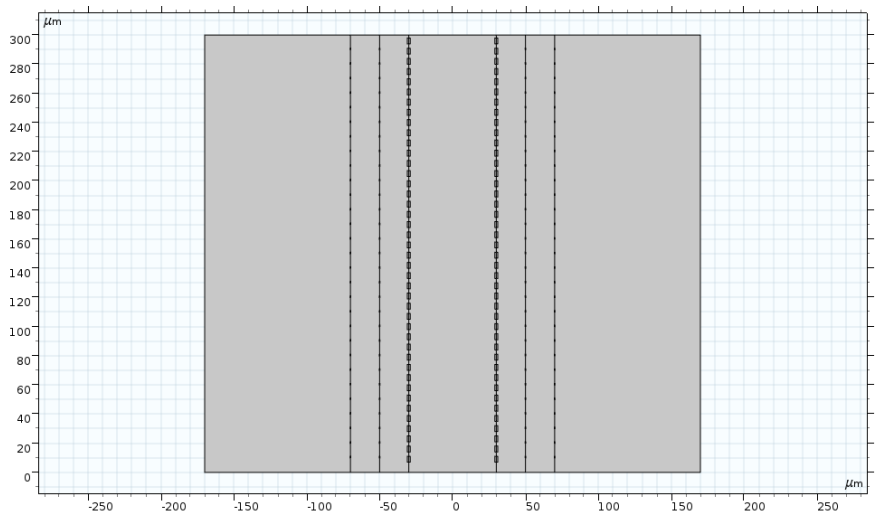

Figure S11. 2D geometry of the microstructure of the one-unit sugarcane.

Calculation of the Reynolds number (R_e) follows:

$$R_e = \frac{\rho v d_v}{\mu} \quad (1)$$

where ρ is the density of the fluid (SI units: kg/m^3); v is the velocity of the fluid with respect to the object (m/s); d_v is a characteristic linear dimension (m); μ is the dynamic viscosity of the fluid (Pa·s or N·s/m^2 or kg/(m·s)). Evaporation occurs from the top surface of the sugarcane

with an evaporation rate (E_{ev}) of 1.31 kg·m^{-2}·h^{-1} ≈ 0.00036 kg·m^{-2}·s^{-1} (for 1 sun). E_{ev} can be related to the water removal speed (v_{ev}): $v_{ev} = E_{ev}/\rho_w$ =3.64×10^{-7} m·s^{-1}; ρ=10^3 kg/m^3; for the vascular bundle, the d_v=60 μm; the μ=0.89×10^{-3} kg/(m·s).

For the vascular bundle, the Reynolds number is:

$$R_e=\frac{10^3\times3.64\times10^{-7}\times60\times10^{-6}}{0.89\times10^{-3}}=2.45\times10^{-5};$$

Compared to the vascular bundle, for pores in the wall of the parenchyma cells, the d_v =1 μm; meanwhile, the v in the position of the pore tends to zero, thus, the Re tends to be infinitely small and the flow resistance coefficient tends to infinity.

The very low Reynold number allows us to use a laminar flow model for fluid flow analysis. The steady and incompressible, laminar flow can be shown with the Navier-Stokes equations:

$$\nabla\cdot\mathbf{u}=0 \quad (2)$$

$$\rho(\mathbf{u}\cdot\nabla)\mathbf{u}=\nabla\cdot[-\mathrm{p}\mathrm{I}+\mu(\nabla\mathbf{u}+(\nabla\mathbf{u})^{\mathrm{T}})]+\mathrm{F} \quad (3)$$

where **u** is the flow velocity vector, p is the pressure, ρ and μ are the density and the dynamic viscosity of water, respectively. F is body force which can be ignored there.

We set the average outlet velocity as 0.36 μm s^{-1} on the top surface and the bottom surface is set at a constant hydrostatic pressure. The vascular bundle was filled with water while the parenchyma cells was filled with air in the primary. The boundaries were set as the cellulose with the thickness of 2 μm. There were some pores distributed in the inner wall of the cellulose. We use the heat transfer in fluid model to analysis the temperature distribution which can be described in following equation:

$$d_z\rho C_P u\cdot\nabla T+\nabla q=d_zQ+q_0+d_zQ_p+d_zQ_{vd} \quad (4)$$

$$\rho C_P u\cdot\nabla T-\nabla(k\nabla T)=q_0 \quad (5)$$

where the ρ, C_p and T are the mass density, liquid thermal capacity and the temperature, respectively; u and k is the fluid flow speed and thermal conductivity of the aqueous medium; q_0 represents the thermal energy input from the optical-thermal conversion. The Multiphysics simulations are conducted by COMSOL Multiphysics 5.3a, under the steady analysis mode. Wherein, a constant heat flux of 0.2 kW m^{-2} occurs on the top surface, corresponding to the solar energy input on the surface of sugarcane (the evaporation consumed the energy of ca 0.8 kW m^{-2}). To carry out a qualitative analysis, we assume that the temperature of environment and water was set to 25 ºC (298.15 K); the balanced heat flux was 0.2 kW m^{-2}. The water flow velocity distribution and temperature distribution of the sugarcane with one unit were shown in Figure S12.

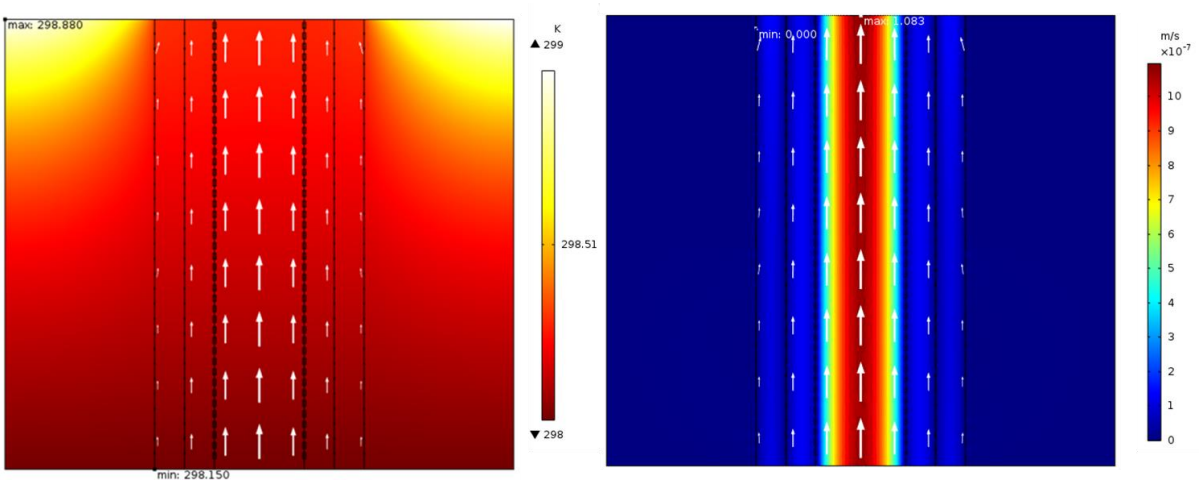

Figure S12. Flow velocity of water and temperature distribution of the sugarcane with one unit.

The distribution of the temperature and velocity will not change along the horizontal direction (Figure S13 and S14). However, for the temperature, its distribution is not gradient in the vertical section. So the sugarcane with one unit could not truly represent the actual temperature distribution of the sugarcane.

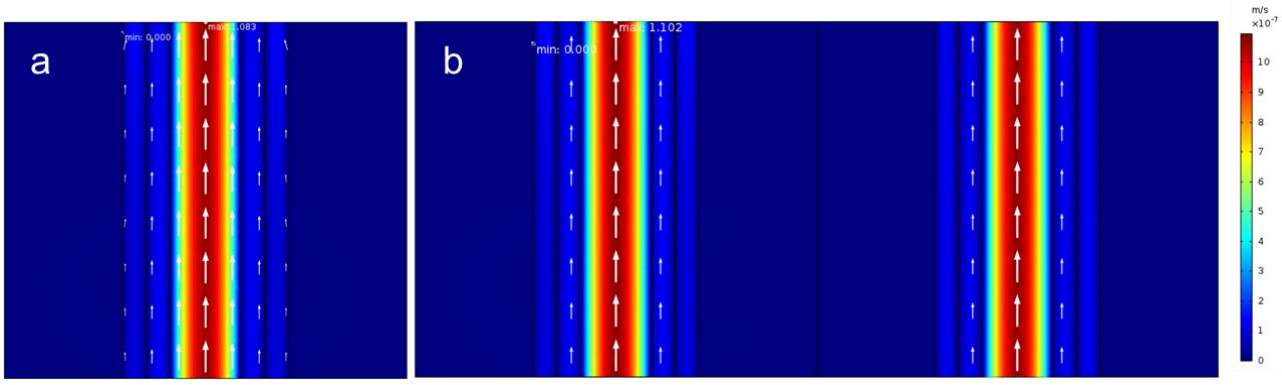

Figure S13. Steady state simulation of flow velocity distribution in (a) one unit and (b) two units along the horizontal direction.

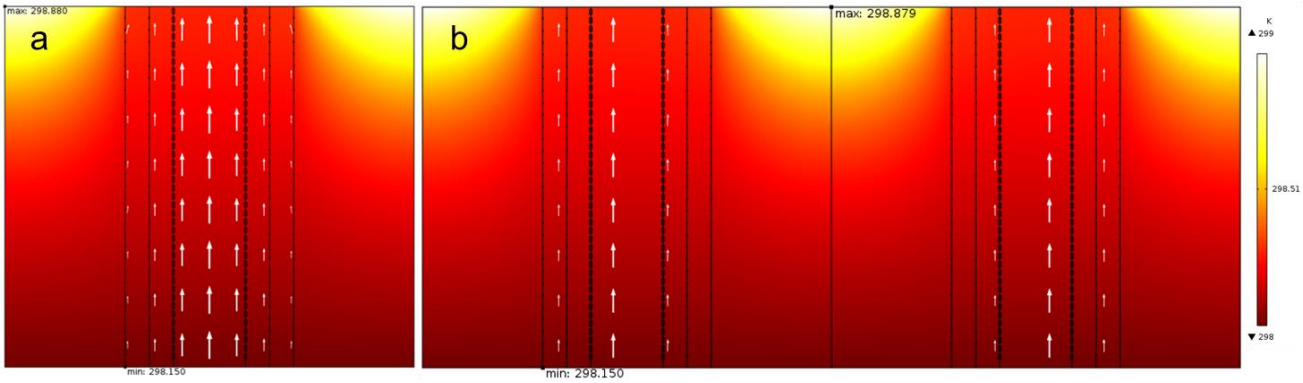

Figure S14. Steady state simulation of temperature distribution in (a) one unit and (b) two units along the horizontal direction.

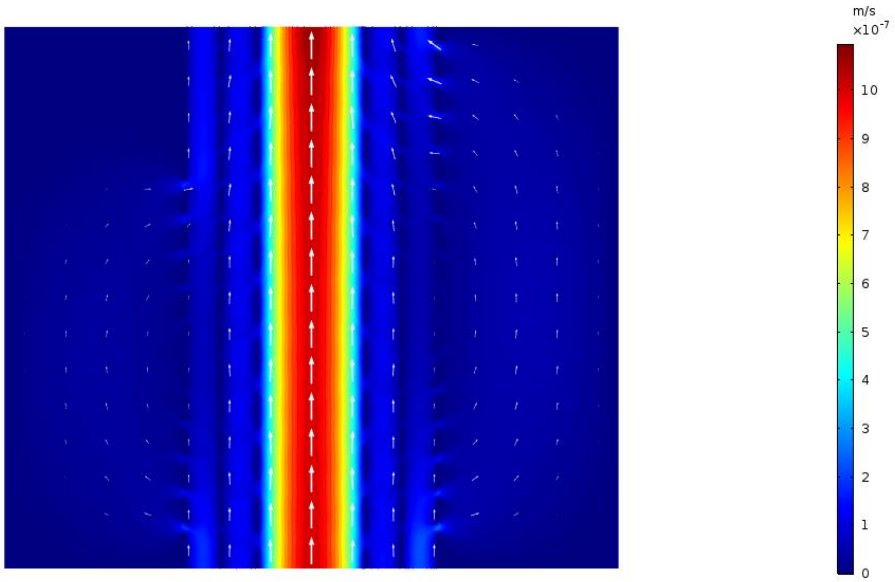

Figure S15. Simulation of the flow velocity distribution with the pore size in the inner wall of the parenchyma cell increased to 5 μm.